

Efficient one-pot conversion of cellulose into sorbitol with Ru-doped chitosan-phytic acid supramolecular crosslinked catalyst

Yingqiao Zhou^a, Richard L. Smith Jr^b, Xinhua Qi^{a,*}

^a College of Environmental Science and Engineering, Nankai University, No. 38, Tongyan Road, Jinnan District, Tianjin 300350, China

^b Graduate School of Environmental Studies, Tohoku University, Aramaki Aza Aoba 468-1, Aoba-ku, Sendai 980-8572, Japan



ARTICLE INFO

Keywords:

Biomass
Cellulose
Hydrolytic hydrogenation
Sorbitol
Nitrogen and phosphorus co-doped

ABSTRACT

Bifunctional catalysts synthesized from renewable materials for conversion of cellulose to platform chemicals are needed in biorefinery development. Herein, supramolecular assembly and crosslinking of chitosan by phytic acid was used to synthesize Ru-doped phosphorus- and nitrogen- carbon catalysts (Ru/PNC) for one-pot conversion of cellulose to sorbitol. Sorbitol yields as high as 78% were obtained from cellulose with the Ru/PNC catalyst in water at 200 °C and 4 MPa H₂ for 3 h. P content was found to have a linear relationship with the cellulose conversion and sorbitol yield within a certain range. The prepared catalyst exhibited good stability, and could be recycled for at least 5 times. Other cellulosic sources (cotton wool, filter paper) afforded sorbitol yields >60%, showing the potential of the catalyst for industrial production. This work demonstrates that supramolecular assembly and cross-linking can be used to design efficient, durable, and renewable bifunctional catalysts for biomass upgrading.

1. Introduction

Biomass conversion is playing an increasing important role in energy and industry for promoting sustainable development [1]. Cellulose, which is the chief constituent of biomass, is expected to serve as raw material for society's future needs for chemical and healthcare products [2]. As a multifunctional compound, sorbitol has a wide range of applications and a huge market demand [3]. Catalytic conversion of lignocellulose into the platform chemical sorbitol will become one of the key routes for chemical industry [4]. Traditionally, the conversion of cellulose requires multiple steps involving pretreatment [5], hydrolysis [6], reduction [3,7] and any number of intermediate separation or purification steps. Moreover, typical catalytic processes for conversion of cellulose to sorbitol have unwanted side reactions, such as dehydration, retro-aldol condensation or polymerization [8] reactions that increase complexity of separation and product cost. Design of bifunctional catalysts that have both acidity and hydrogenation activity to allow one-pot conversion of cellulose to sorbitol can resolve these issues.

Ever since Fukuoka and Dhepe reported on a method for converting cellulose into sorbitol in one pot [9], many advanced systems for sorbitol production have been proposed. The combination of liquid acids such as phosphoric acid and sulfuric acid with hydrogenation catalysts such as

Ru/C and Raney nickel have obtained sorbitol yields of more than 50% from cellulose [10]. Deng et al. [11] reported that after pretreating cellulose with phosphoric acid, cellulose was converted into sorbitol with yields of 69% on a Ru/CNT catalyst at hydrogen partial pressure of 5 MPa and a reaction temperature of 185 °C. However, to avoid corrosion by liquid acids and intensive recycle and waste disposal steps, heterogeneous solid acids are needed to depolymerize cellulose [10,12]. Using a solid acid/metal catalyst system, cellulose can be efficiently converted into polyols through hydrolysis by H⁺ ions reversibly-formed by a solid acid in hot water and by hydrogenation on the metal sites [13]. To overcome the limitation of heterogeneous catalysis in solid-solid reactions, the issue of initial contact/affinity between the solid acid and cellulose along with the presence of water must be addressed. High-temperature-resistant solid acid carriers have been commonly used that are loaded with hydrogenation metal sites (Ru, Ni) to form bifunctional catalysts, such as Ni/NCC-ZSM5 [14], Ni/ZrP_x [15], Ru/CsHPA [16], Ru-PW/ZrO₂ [17], Ni-Ru@MC [18]. Although there is good progress in development of catalytic systems, it is still a challenge to design a catalyst that balances acidity activity and hydrogenation activity for obtaining selective conversion of cellulose. Carbon carriers have attracted much attention due to their low cost, stability under hydrothermal conditions and ease at which functional or acidic groups

* Corresponding author.

E-mail address: qixinhua@nankai.edu.cn (X. Qi).

can be grafted onto the material to form solid acid supports [19]. Ribeiro et al. [20] prepared a Ru catalyst Ru/AG-CNT1200 supported catalyst from hydrothermal carbonization (HTC) of a glucose/carbon nanotube mixture. Under reaction conditions of 205 °C and hydrogen partial pressure of 5 MPa, complete conversion of cellulose was achieved in 3 h in which the highest sorbitol yield reported was 64.1%. Li et al. [21] introduced sulfonic acid groups to carbon carriers to prepare Ru/CCD-SO₃H, which enhanced the acidity and promote hydrolysis. Under reaction conditions of 180 °C and hydrogen partial pressure of 4 MPa, a sorbitol yield of 63.8% from cellulose was achieved in 10 h reaction time. Some studies have suggested that phosphoric acid groups have higher selectivity for conversion of cellulose into glucose than sulfonic acid groups [22,23]. For example, a P@HRCBC solid acid rich in -OH and -PO₃H₂ was proposed for cellulose hydrolysis and under reaction conditions of 200 °C and 120 min reaction time, glucose yields of 47.1% were achieved [24]. However, the grafting of sulfonic or phosphate groups onto carbon carriers requires concentrated acids making it difficult to control the number of acidic sites on the surface of the carbon supports [21,25,26]. Furthermore, the subsequent addition of metal sites to carbon supports that does not disturb the acidic sites makes method development tedious.

Chitosan (CS), which naturally contains nitrogen elements, and phytic acid (PA), which has six phosphate groups and is highly hydrophilic, are widely present in nature [27]. It has been reported that CS has strong electrostatic and hydrogen bonding interactions with PA [28], as well as strong coordination ability, which can be used to adsorb heavy

metal ions [29]. Chitosan and phytic acid form a well-constructed supramolecular structure through electrostatic interaction and abundant hydrogen bonding network, which make the proportion and number of heteroatoms, flexible and adjustable, and gives the configurations considerable engineering potential [30]. Phytic acid not only provides the phosphorus source for materials, but also promotes uniform distribution of metal precursors and inhibits the agglomeration of metals [31,32].

Herein, a low-effort method is achieved for synthesis of a nitrogen- and phosphorus- containing Ru-doped structured carbon materials by exploiting strong interactions between chitosan and phytic acid for precise control of acidity and hydrogenation sites of a bifunctional catalyst denoted as Ru/PNC. The versatility of the method is demonstrated by applying the Ru/PNC bifunctional catalyst to achieve selective one-pot conversion of cellulose to sorbitol.

2. Experimental

2.1. Materials

Microcrystalline cellulose was purchased from ACROS. Glucose, sorbitol, RuCl₃·3 H₂O, and phytic acid (PA, 70%) were purchased from Aladdin Chemistry Co. Ltd. Chitosan and cellobiose were purchased from Sigma-Aldrich Chemical Co., Ltd. Ethanol was purchased from Bohua Chemical Reagent Company. All chemical reagents were analytical pure and were used directly.

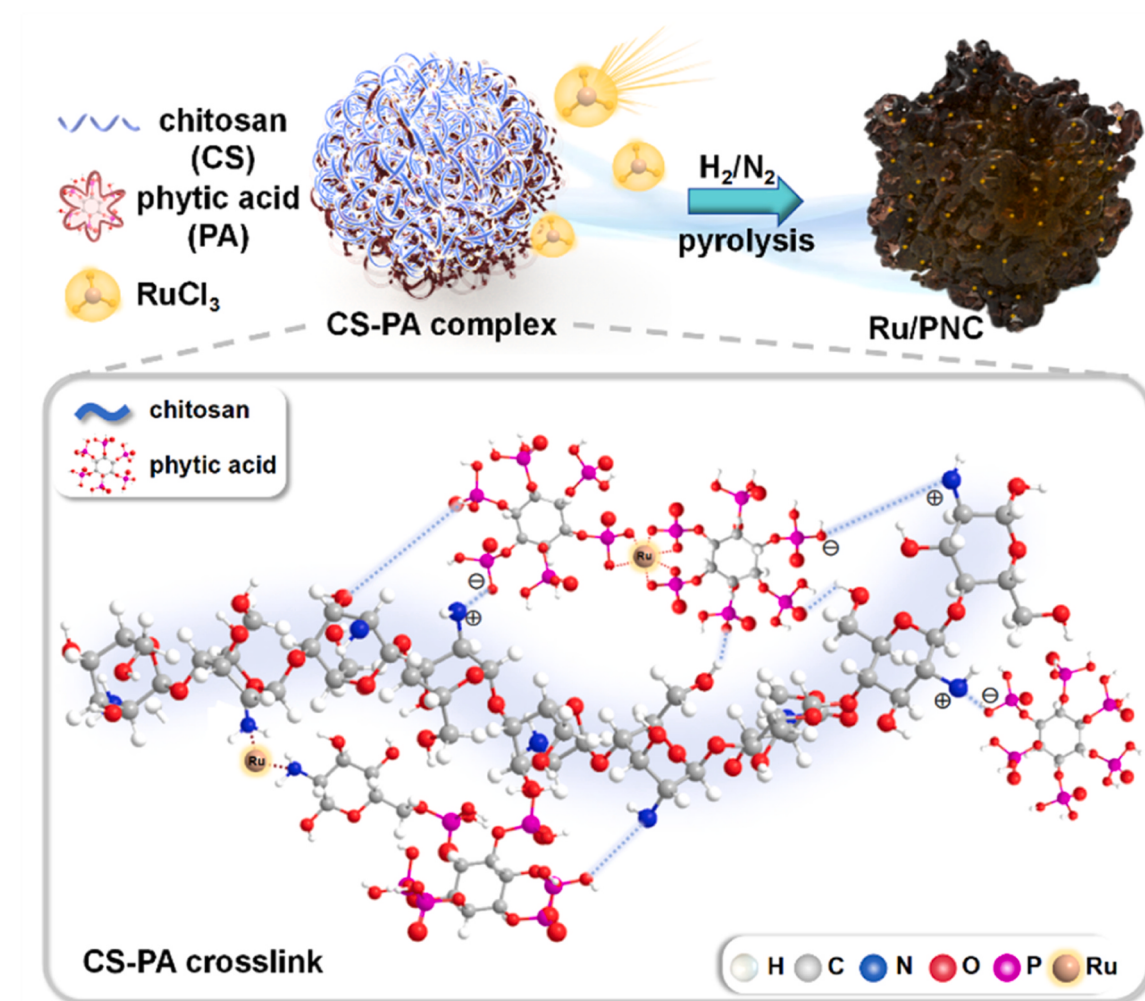


Fig. 1. Schematic illustration of supramolecule crosslinking of chitosan (CS) by phytic acid (PA) and synthesis process of Ru-doped P-N-carbon catalyst (Ru/PNC).

2.2. Synthesis of Ru/PNC

The method for synthesis of Ru/PNC has several key steps (Fig. 1). Typically, chitosan (CS) (0.25–1.75) g was added to 50 mL of ultrapure water with acetic acid additive to form a hydrogel. Phytic acid (PA) (0–1.5) g was dissolved in 40 mL of water and was added dropwise to the chitosan solution, and a white precipitate was formed denoted as CS-PA. A certain amount of RuCl_3 aqueous solution (0.5 wt% to 1.5 wt%, 10 mL) was slowly added to the CS-PA complex and stirred for 24 h at room temperature. During this time, Ru ions in the water became trapped in the cross-linked complex which was then filtered and dried, and the complex of chitosan and phytic acid adsorbed Ru^{3+} was denoted as Ru-CS-PA composite material. The Ru-CS-PA composite material was then heated to an appropriate temperature (400 °C, 550 °C, 700 °C) with a heating rate of 2 °C·min⁻¹ and maintained for 2 h under a flowing 5% H_2/N_2 (vol/vol) atmosphere. The obtained materials were washed three times with deionized water and dried in a vacuum oven at 60 °C for 6 h. The final catalytic materials were denoted as Ru/P(x)NC-y, where x (wt %) represents the mass percentage of P in the catalyst measured by ICP and y (°C) represents the heat treatment temperature. For comparison, control samples denoted as Ru/NC and PNC were prepared at 550 °C as the above procedure but without adding phytic acid or $\text{RuCl}_3 \cdot \text{xH}_2\text{O}$, respectively.

2.3. Characterization

Material morphology and elemental distribution were examined with scanning electron microscopy (Zeiss sigma-300) and transmission electron microscopy (TALOS F200). Powder X-ray diffraction (XRD) patterns were measured with a Rigaku Ultima IV diffractometer (give source and power specifications). X-ray photoelectron spectroscopy (XPS) was performed with a Thermo Fisher Escalab 250x instrument. N_2 adsorption/desorption isotherms were measured on a Micromeritics ASAP 2460 instrument using N_2 at –196 °C. Specific surface area (S_{BET}) and pore size distributions were obtained from desorption isotherms using the Brunauer-Emmett-Teller (BET) method and Barrett-Joyner-Halanda (BJH) model, respectively. FT-IR spectra were collected using a Nicolet IS50 spectrometer. TGA analyses were conducted on a Jupiter STA 449 F5 thermoanalyzer. Metal loading of catalysts was determined with inductively coupled plasma optical emission spectroscopy (ICP-OES) on an Agilent 730 spectrometer. Characterization of Brønsted and Lewis acid sites of the materials was determined with FTIR (Nicolet 380 Fourier Transform Infrared Spectrometer) using pyridine (Py) as a probe molecule. NH_3 temperature-programmed desorption ($\text{NH}_3\text{-TPD}$) was used to determine the acidic strength of materials and was carried out on an Autochem II 2920 instrument.

2.4. Catalytic experiments

Cellulose was ball-milled for (1–3) h at 300 rpm with a Retsch PM100 planetary ball mill equipped with ceramic pots (30 mL) loaded with twelve ZrO_2 balls of different sizes (6 mm and 8 mm of diameter). Cellulose and catalyst were mix ball-milled (isothermal) according at a given proportion as pre-treatment to improve the contact between cellulose and the catalyst.

In a typical experiment, 0.5 g cellulose and 0.2 g catalyst were added into the pot and ball-milled at 300 rpm for 3 h prior to reaction, to obtain a cellulose catalyst mixture with a mass ratio of 5:2. Then, 0.07 g of the solid mixture and 5 mL of ultra-pure water were added to a Teflon-lined steel autoclave. The amount of the solid mixtures added was changed according to the different proportions used to ensure a cellulose content of 0.05 g. In experiments that used glucose or cellobiose as alternate substrates for cellulose, 1 wt% glucose or 1 wt% cellobiose aqueous solution (5 mL) and 0.02 g Ru/PNC catalyst were added to the autoclave.

Before each run, the autoclave was purged with hydrogen gas three

times to remove the air prior to applying 4 MPa H_2 partial pressure to the system. The autoclave was then heated to a given temperature (180–210) °C and maintained at that condition for a given reaction time. To terminate the reaction, the autoclave was cooled and the filtrate of each reaction solution was analyzed with a high-performance liquid chromatograph (HPLC) having a refractive index detector (Agilent 1260 Infinity II). An HPLC column of Aminex HPX-87 H (7.8 mm × 300 mm) was used at 50 °C column temperature with 0.005 M sulfuric acid aqueous solution at a flow rate of 0.5 mL·min⁻¹ as mobile phase. To distinguish between sorbitol and mannitol, liquid products were re-analyzed by HPLC (Waters e2489) equipped with an RI detector and a SC1011 column at 60 °C, with H_2O as the mobile phase at a flow rate of 0.5 mL·min⁻¹. For determining the conversion of cellulose, total organic carbon (TOC) amounts contained in the resultant liquids were obtained with a Multi N/C 3100 TOC analyzer. Each experiment was repeated at least three times to ensure reproducibility. Product yields, cellulose, cellobiose and glucose conversions were calculated according to Eqs. (1–3):

$$\text{Cellulose conversion (\%)} = \frac{\text{mass of total organic carbon in solution}}{\text{mass of carbon in initial cellulose}} \times 100\% \quad (1)$$

$$\text{Yield (\%)} = \frac{\text{mass of carbon in sorbitol formed}}{\text{mass of carbon in initial substrate}} \times 100\% \quad (2)$$

$$\begin{aligned} \text{Cellobiose or glucose conversion (\%)} \\ = 1 - \frac{\text{final mass of cellobiose or glucose}}{\text{initial mass of cellobiose or glucose}} \times 100\% \end{aligned} \quad (3)$$

3. Results and discussion

3.1. Synthesis and characterization of Ru/PNC

Supramolecule assembly and synthesis of Ru/PNC can be understood through an image (Fig. 1) that shows the crosslinking process that occurs through presence of an abundant number of phosphate groups from phytic acid interacting with chitosan amine and hydroxyl groups through electrostatic and hydrogen bonding interactions as confirmed by FTIR analyses (Fig. S1). Characteristic peaks at (3200–3600) cm^{-1} belonging to the stretching vibration of the $-\text{NH}_2$ or $-\text{OH}$ group in CS, and at 1385 cm^{-1} belonging to the stretching vibration of C-N in CS were observed (Fig. S1). The $-\text{OH}$ and $-\text{NH}_2$ peaks in the CS-PA complex were red-shifted (Fig. S1), while a new N-O stretching vibration peak appeared at 1540 cm^{-1} (Fig. S1). In addition, polyelectrolyte conjugation and precipitation occurred due to strong electrostatic interactions between negatively charged phytic acid and positively charged chitosan [33]. The amine group of chitosan and the phosphate group of phytic acid can form coordination bonds with heavy metal ions that can trap and hold Ru^{3+} , thus the CS-PA composite has strong adsorption capacity for ions [31]. After the addition of Ru^{3+} , the $-\text{OH}$, $-\text{NH}_2$ and $\text{P}=\text{O}$ bond peaks in the FTIR spectrum of the Ru-CS-PA complex (Fig. S1) became blue shifted confirming the coordination of Ru^{3+} with CS-PA complex. The Ru-CS-PA mixture was subsequently dried and thermally reduced to form the Ru-doped phosphorus- and nitrogen-containing carbon catalyst (Ru/PNC). During pyrolysis, the CS-PA composite network promoted dispersion of Ru, while N and P groups became incorporated into the carbon framework (Fig. 1) as shown by analyses explained next.

SEM (Figs. S2–S3) and TEM (Figs. 2a–2b) images show the morphology and structure of as-prepared Ru/PNC-550 samples. SEM images (Figs. S2a–S2b) showed that the samples appeared as irregular sponge blocks of (2–15) μm in particle size with rough surfaces. TEM images (Fig. S3) of Ru/PNC showed that particles had rough ripple-like porous surface structures. Ru nanoparticles in Ru/PNC-550 were well-dispersed (Fig. 2a) with an average diameter of *ca.* 3.8 nm. The

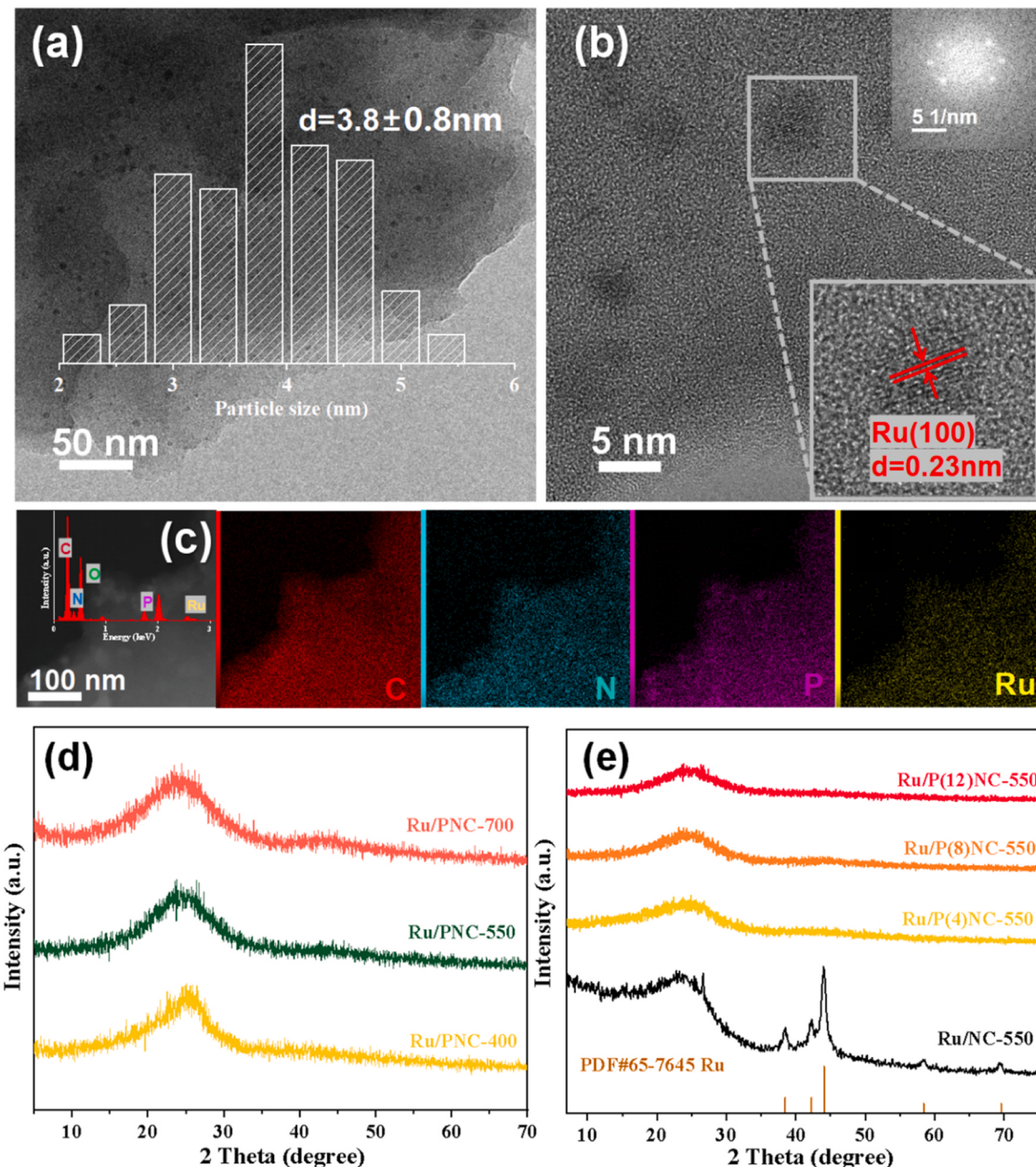


Fig. 2. Morphology and characterization of Ru-doped phosphorus- and nitrogen- carbon catalysts (Ru/PNC- y), y = pyrolysis temperature used in preparation: (a) TEM image of Ru/PNC-550 with corresponding Ru particle size statistics. (b) HR-TEM image with fast Fourier transform pattern showing Ru lattice fringes; (c) TEM-EDS elemental mappings of C, N, P, Ru with EDS spectra (inset). XRD patterns of (d) Ru/PNC- y ($y = 400 \text{ }^{\circ}\text{C}, 550 \text{ }^{\circ}\text{C}, 700 \text{ }^{\circ}\text{C}$) and (e) Ru/P(x)NC ($x = 0, 4, 8, 12$), x = phosphorus content used in preparation.

particle size of Ru increased slightly at higher preparation temperatures (Ru/PNC-400: *ca.* 2.6 nm; Ru/PNC-550: *ca.* 3.8 nm; Ru/PNC-700: *ca.* 4.3 nm), indicating that phytic acid does indeed contribute to metal dispersion (Fig. S4). High-resolution TEM (HRTEM) images (Fig. 2b) clearly showed typical lattice fringes of Ru [34]. It can be observed that C, N, P and Ru were homogeneously distributed in the Ru/PNC samples through the elemental mapping and EDS spectra (Fig. 2c).

XRD patterns of the Ru/PNC- y ($y = 400 \text{ }^{\circ}\text{C}, 550 \text{ }^{\circ}\text{C}, 700 \text{ }^{\circ}\text{C}$) and Ru/P(x)NC-550 ($x = 0, 4, 8, 12$) catalysts are shown in Figs. 2d-2e. Characteristic peaks of Ru or Ru phosphides for a series of Ru/PNC materials did not appear in the XRD patterns for either samples having different phytic acid dosages or samples treated at different calcination temperatures, which may be due to the uniform distribution of Ru or the formation of amorphous alloys. A series of Ru/PNC catalysts showed a

broad diffraction peak at about 20° to 30° , which can be attributed to amorphous carbon [35]. No diffraction peaks corresponding to Ru or metallic phosphides were observed, indicating that the Ru were either highly dispersed or existed in amorphous form of metallic phosphides [36]. In contrast, Ru/NC without phosphorus had sharp characteristic peaks of metal Ru corresponding to the diffraction pattern of Ru (JCPDS 65-7645) [37]. Textural properties and surface composition of Ru/P(x)NC- y are summarized in Table S1. Specific surface areas calculated by N_2 adsorption-desorption isotherms using the Brunauer-Emmett-Teller (BET) method of Ru/PNC-400, Ru/PNC-550 and Ru/PNC-700 showed that all samples had low specific surface areas.

Survey scan XPS indicated the presence of C, O, P, N and Ru elements (Fig. 3a) in Ru/PNC- y samples and surface atomic compositions (Table S1) showed that all Ru/P(x)NC- y catalysts were mainly composed

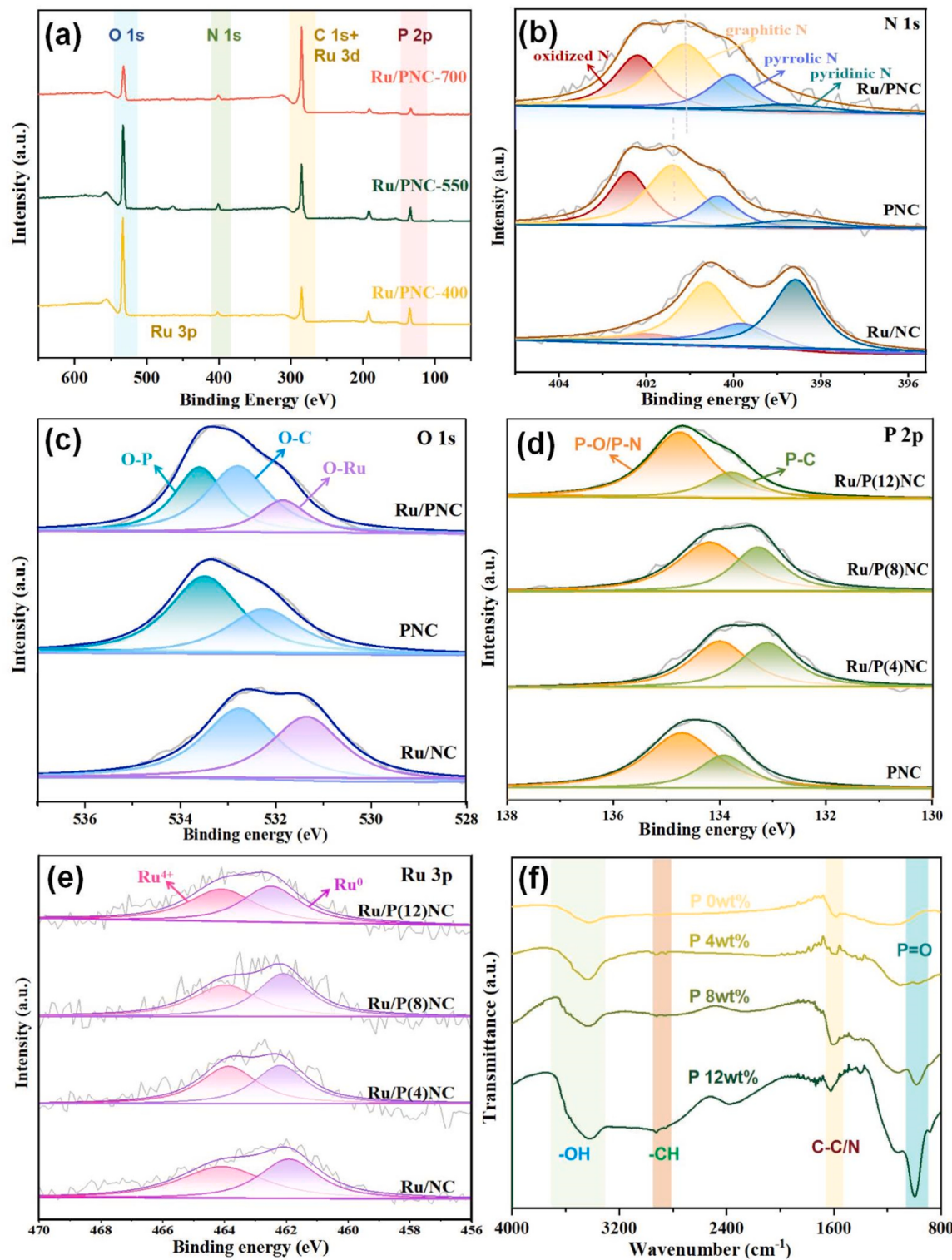


Fig. 3. XPS and FTIR spectra of Ru/P(x)NC-y: (a) Total XPS spectra of Ru/PNC-y ($y=400$ °C, 550 °C, 700 °C), y = pyrolysis temperature used in preparation; (b-d) high-resolution XPS spectrum for Ru/PNC, PNC and Ru/NC of: (b) N 1 s, (c) O 1 s; (d) high-resolution XPS spectrum for Ru/P(x)NC and PNC of P 2p; (e) high-resolution XPS spectrum of Ru 3p for Ru/P(4–12)NC and Ru/NC; (f) FT-IR spectrum of Ru/P(x)NC, x =P wt% in catalyst.

of C, O and P elements. The doping of high electronegativity N ($\chi=3.04$) and low electronegativity P ($\chi=2.19$) synergistically has an electronic modulation effect on carbon supported metal catalysts and affects the electronic structure of the loaded metal [38]. As shown in Fig. 3b, the N 1 s spectrum can be deconvoluted into multiple peaks at (398.2, 399.8, 401.4, 402.5) eV attributed to (pyridinic-N, pyrrolic-N, graphitic-N,

oxidized-N), respectively [33]. These nitrogen species impart specific chemical/electronic environments to neighboring carbon atoms that results in different catalytic activities. The peak values of N 1 s in Ru/PNC were red-shifted relative to PNC supports, which further confirms the transfer of electrons from Ru to N suggesting strong Ru-N interactions. Phosphorus incorporation resulted in a sharp decrease in

pyridine nitrogen content (i.e. Ru/NC: 40.6%, Ru/PNC: 9.4%), which hinders of cellulose hydrolysis [39]. All samples had a broad peak for O1s (Fig. 3c) corresponding to C-O (532.3 eV). Compared with PNC, the generated Ru-O peak (531.7 eV) due to addition of Ru caused the O1s spectrum to shift to lower energies (Fig. 3c). Compared with Ru/NC, the overall O1s peak of Ru/PNC was shifted to higher energy in the phosphorus-containing material due to the introduction of O-P bonds (533.6 eV) [31]. Therefore, a series of catalysts with varied P content were prepared to study the effect of heteroatom doping on the chemical bonding energy of surface elements. The P 2p spectrum of Ru/PNC (Fig. 3d) was deconvoluted into two peaks at 134.5 eV and 133.8 eV corresponding to P-C and P-O/P-N, respectively [40]. The P 2p peak shifted towards higher binding energies with an increase in P content, indicating an increase in phosphorus valence, the formation of electron-deficient P with stronger Lewis acidity. There was no apparent Ru-P bonding given in the XPS spectra or XRD patterns (Figs. 2d-2e), probably because Ru clusters are more easily adsorbed around defective N sites compared with P sites, which caused uniform distribution of Ru clusters and limiting the aggregation of metal atoms during high temperature pyrolysis (Fig. 2d, Fig. S4) [35]. Considering that the binding energy of Ru 3d peak partially overlaps with the C 1s peak, the Ru 3p region was selected for measuring the state of metal Ru [41]. The XPS peak of Ru⁰ shifted toward high binding energies with increasing P content (Fig. 3e), which indicated interaction of Ru with phosphorus and the tendency of Ru to keep the relative electron-rich state of Ru atoms on surface of the material which is favorable for catalytic hydrogenation [42].

FT-IR measurements made on Ru/P(x)NC-550 catalysts (Fig. 3f) showed stretching vibration of -OH (3200–3400 cm⁻¹), -CH (~2900 cm⁻¹), and the tensile vibration of C=C/C-N (~1600 cm⁻¹), and P=O (~1170 cm⁻¹) which were in accordance with XPS spectra results. XPS analyses (Table S1) showed that a decrease in P is closely related to a decrease in O, which is in accordance with the presence of phosphate groups on the catalysts surface. Remarkably, with increasing P content, especially P > 4 wt%, more distinct characteristic peaks of phosphate groups moved towards higher wavenumbers (Fig. 3f), which may lead to changes in acidity on the catalyst surface [15]. Contact angles of Ru/PNC and Ru/NC materials (Fig. S5) were 15.7° and 144.4°, respectively, indicating that phosphorus greatly increased the hydrophilicity of the carbon surface.

Table 1

Conversion of cellulose to sorbitol over synthesized Ru/P(x)NC-y catalysts^a, x= P content used in preparation, y= pyrolysis temperature in °C used in preparation.

Entry	Catalyst	Ru content (wt %) ^b	P content (wt %) ^b	Cellulose conversion (%)	Sorbitol yield (%)	Glucose yield (%)	Major by-products ^c (%)
1	no catalyst	-	-	28.7	0	5.1	n.d.
2	PNC	-	8.9	88.1	0	50.8	n.d.
3	Ru/PNC-400	3.5	12.3	77.6	46.4	8.5	isosorbide (5.4), C5 sugar alcohols (2.2), mannitol (0.8)
4	Ru/PNC-550	3.1	10.4	92.3	78.5	0	C5 sugar alcohols (3.1), mannitol (2.8), isopropanol (0.4)
5	Ru/PNC-700	3.1	9.1	81.6	66.3	0.3	C5 sugar alcohols (4.7), isopropanol (2.3), mannitol (1.1)
6	Ru/P(4)NC-550	3.4	3.9	68.5	48.7	2.2	C5 sugar alcohols (1.7), mannitol (1.0), isopropanol (0.3)
7	Ru/P(8)NC-550	3.5	8.6	83.9	55.3	4.6	n.d.
8	Ru/P(12)NC-550	2.8	12.1	93.3	78.1	0.1	C5 sugar alcohols (2.9), mannitol (2.6), isopropanol (0.6)
9	Ru/P(16)NC-550	3.0	15.8	100	57.6	5.4	isosorbide (7.2), C5 sugar alcohols (1.2), 5-HMF (0.2)
10	Ru/NC-550	3.0	-	30.1	6.8	0	C5 sugar alcohols (1.5), isopropanol (0.5)

^a Reaction conditions: 50 mg ball-milled cellulose, 20 mg catalyst (mix-milled with cellulose), 5 mL pure water, 200 oC reaction temperature, 4 MPa partial pressure H₂, 3 h reaction time.

^b Actual loading of Ru and P in catalyst determined by ICP-OES analysis.

^c C5 sugar alcohols arabinitol or xylitol detected by HPLC.

^d n.d.: not detected.

3.2. Catalytic conversion of cellulose to sorbitol by Ru/PNC catalysts

3.2.1. Influence of catalyst properties

Catalytic conversion of cellulose to sorbitol over the synthesized materials was investigated as one-pot batch reactions (Table 1). In control experiments with no catalyst (Entry 1, Table 1), the cellulose underwent hydrolysis due to the hydrothermal conditions to give a cellulose conversion of 28.7% and a glucose yield of 5.1%. No sorbitol was formed over PNC (Entry 2, Table 1), however a glucose yield of 50.8% was observed, suggesting that active acidity sites were present on the PNC material.

NH₃-TPD (Fig. 4a) and Py-IR (Fig. 4b) measurements (Table S2) showed that the total number of acid sites were proportional to phosphorus content and the sites had a Brønsted/Lewis site (B/L) ratio of about 0.1. NH₃ desorption peaks (Fig. 4a) observed at relatively low temperatures (<200 °C) can be attributed to physical adsorption or weakly acidic sites (e.g. -OH and -COOH), while broad desorption peaks between 300 °C and 600 °C correspond to active sites of medium acidity which are attributed to acids originating from the -PO₄H₂ group and Ru-N_x interactions or defects.

The acid strength and acid amount of Ru/P(x)NC-ys are calculated and summarized in Table S2. The NH₃-TPD profiles of the materials calcined at different temperatures are compared in Fig. 4a. It can be observed that the samples with a lower calcination temperature (400 °C) show a higher proportion of weak acid sites, while the materials calcined at 550 and 700 °C show mainly medium-strong acids, which may be due to the destruction of weak acid groups at high temperatures. The conversion of cellulose to sorbitol using catalysts prepared at different calcination temperatures was studied. The results are shown in Table 1, and the highest sorbitol yield was achieved at a calcination temperature of 550 °C. The Ru/PNC-400 catalyst prepared at 400 °C was not conducive to the reduction and exposure of hydrogenation sites, producing byproducts such as glucose and isosorbide (Table 1, Entry 3). The Ru/PNC-700 catalyst prepared at 700 °C lost acidic sites due to the high preparation temperature, resulting in a lack of hydrolysis ability and a lower cellulose conversion (Table 1, Entry 5). Brønsted and Lewis surface acidity of Ru/PNC-550 was analyzed by IR-spectroscopy using pyridine as the probe molecule (Fig. 4b). The peak at 1535–1550 cm⁻¹ can be attributed to Brønsted acid sites, while the peaks at 1530–1550 cm⁻¹ and 1610–1640 cm⁻¹ refer to Lewis acid sites [43]. The spectral band at 1480–1500 cm⁻¹ is related to the vibration of the

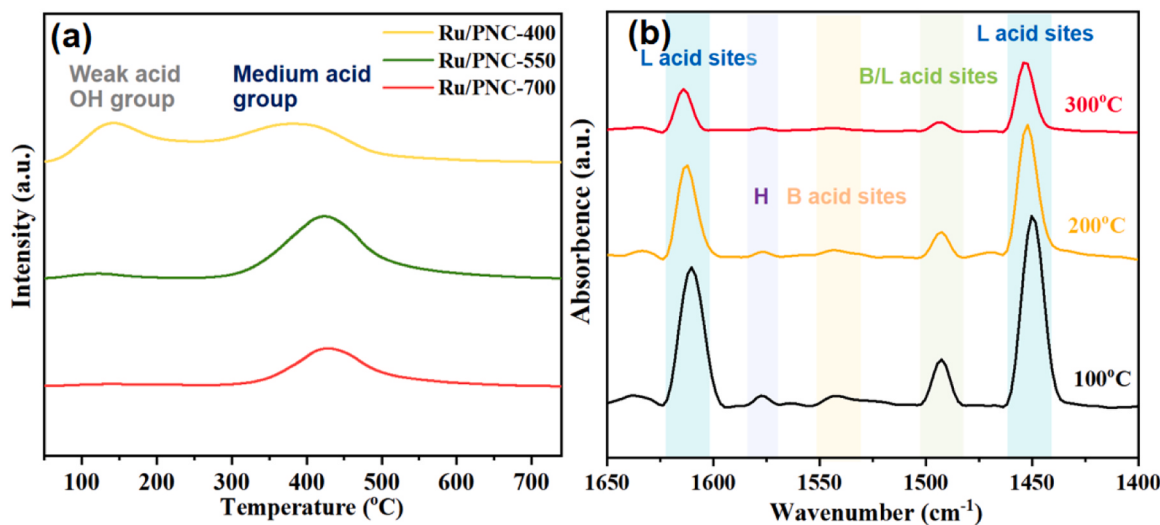


Fig. 4. (a) NH₃-TPD profiles of Ru/PNC- y ($y=400, 550, 700$) catalyst; (b) Py-IR spectra of Ru/P(12)NC-550 at (100, 200, 300) °C.

pyridine ring on both Brønsted and Lewis acid sites and an additional hydrogen-bonded adsorption peak was detected at 1575 cm⁻¹ for Ru [43]. It is noteworthy that all catalysts exhibited much higher Lewis acid site amounts than Brønsted acid sites (B/L ratio=0.05–0.12) (Table S2), which means that the incorporation of Ru content and doping of heteroatoms and defects in the catalyst surface resulted in abundant Lewis acid sites [44]. The chemical environment of P atoms in synthetic materials was studied by solid-state NMR (Fig S6), wherein ³¹P NMR spectra showed a clear signal at -1.8 ppm, which belonged to orthophosphate, confirming the existence of surface phosphate groups [45]. Peaks at -14.8 ppm and -53.6 ppm were attributed to different P–O bonds, while the peak at 49.4 ppm was attributed to P(O)–C [45–47]. A small amount of P atoms were doped into the carbon lattice, and the doping of nitrogen also affected the chemical shift of phosphorus, resulting in the appearance of other weaker peaks [48]. With an increase in phosphorus doping, abundant P–C bonds and other defects on the catalyst surface lead to high Lewis acid sites, and P–OH provided Brønsted acid sites, both of which lead to an increase in the number of acid sites.

The relationship between P content and catalytic activity was investigated for materials prepared at a calcination temperature of 550 °C (Table S3). NH₃-TPD profiles of Ru/P(x)NC-550 materials (Fig. S7) showed that increased phosphorus content in the samples materials Ru/P(x)NC resulted in a higher total number of acid sites (Table S2), while the ratio of Brønsted acid sites to Lewis acid sites did not change much (Table S2). When the P content increased from 4 wt% to 14 wt%, the total acidity increased from 1.26 mmol/l to 2.64 mmol/l (Table S2), while the cellulose conversion increased proportionally to the total acidity and sorbitol yield exhibited a maximum at around 12 wt % P content (Fig. S7). When the P content was increased to 16 wt% (Table 1, Fig. S8), cellulose conversion reached almost 100%, but the selectivity of sorbitol decreased and byproducts such as isosorbide were detected (Table 1). Since the cellulose hydrolysis is the rate-limiting step in one-pot conversion of cellulose to sorbitol, positive correlation between cellulose conversion and the number of acid sites was confirmed. However, it became clear in the experiments that sorbitol selectivity decreased for P content greater than 12 wt%, which suggests that surface acidity was an important, but non-exclusive factor for the catalytic performance of Ru/PNC. The influence of Ru content in Ru(z)/P(12)NC-550 catalyst ($z = 1–5$) on cellulose conversion was examined (Fig. S9), where it was found that a minimum of 3 wt% Ru was required for sorbitol yields of at least 60%. In summary, acidity of the catalyst was found to be directly proportional to phosphorus content, thereby affecting hydrolysis, while hydrogenation of glucose formed required a

minimum Ru content of 3 wt%, thus maximum sorbitol yields can be obtained by balancing hydrolysis and hydrogenation active sites in a catalyst [49].

To verify performance the structure-activity relationship of the (hydrolysis-hydrogenation) Ru(3)/P(12)NC-550 material, a series of catalysts with different P content was tested with glucose and cellobiose as substrates (Table S3). When cellobiose was used as substrate (Table S3), sorbitol yield exhibited a maximum with P content similar to results for cellulose conversion, but Ru/P(4)NC showed the best catalytic performance (100% conversion, 94.3% sorbitol yield), most likely because hydrolysis of cellobiose requires fewer acid sites than cellulose. Interestingly, when glucose was used as the substrate (Table S3), low P content in the catalyst or low total acidity gave the highest sorbitol yields, possibly due to the abundant Brønsted or Lewis acid sites promoting the conversion of glucose to humic acid at high-temperatures.¹⁵ Additionally, adsorption experiments (Table S4) showed that the Ru/P(10)NC catalyst had a weaker affinity for sorbitol than for the intermediates glucose and cellobiose, and sorbitol was easily desorbed from the catalyst.

3.2.2. Mechanochemistry of cellulose-catalyst mix-milling

Efficiency of a catalyst for promoting hydrolysis is related to acid strength, type (B or L) and number of catalytic sites, but also depends on proximity of the substrate to the catalytic site and on the presence of water [50,51]. Mass transfer limitations due to contact between a water-insoluble substrate (cellulose) and a solid acid catalyst are widely recognized. Ball-milling pretreatment was applied to decrease the crystallinity of cellulose, to increase the contact between catalyst and cellulose, and to improve mass transfer. XRD patterns of untreated cellulose, ball-milled cellulose, and mix-milled catalyst and cellulose (Fig. S10) showed that samples became amorphous when ball-milled or mix-milled (catalyst:cellulose ratio of 2:5). Changes in FT-IR spectra of samples before and after ball milling were measured (Fig. S11) and showed qualitative weakening. Ball-milling reduced cellulose crystallinity, which in turn promoted hydrolysis of cellulose and hydrogenation of glucose (Fig. 5a). Cellulose reacted without ball-milling pretreatment (untreated cellulose, Fig. 5a) gave sorbitol yields that were around 23% (Fig. 5a), whereas when cellulose was ball-milled, sorbitol yields increased to more than 60% (Fig. 5a). On the other hand, when Ru/P(10)NC-550 catalyst and cellulose were mix-milled together as pretreatment, sorbitol yields reached values as high as 78.1% for 3 h reaction time (Fig. 5a) and yields did not change much when mix-milling time was extended from 3 h to 4 h.

In the mix-milling of catalyst and cellulose, the mass ratio of catalyst

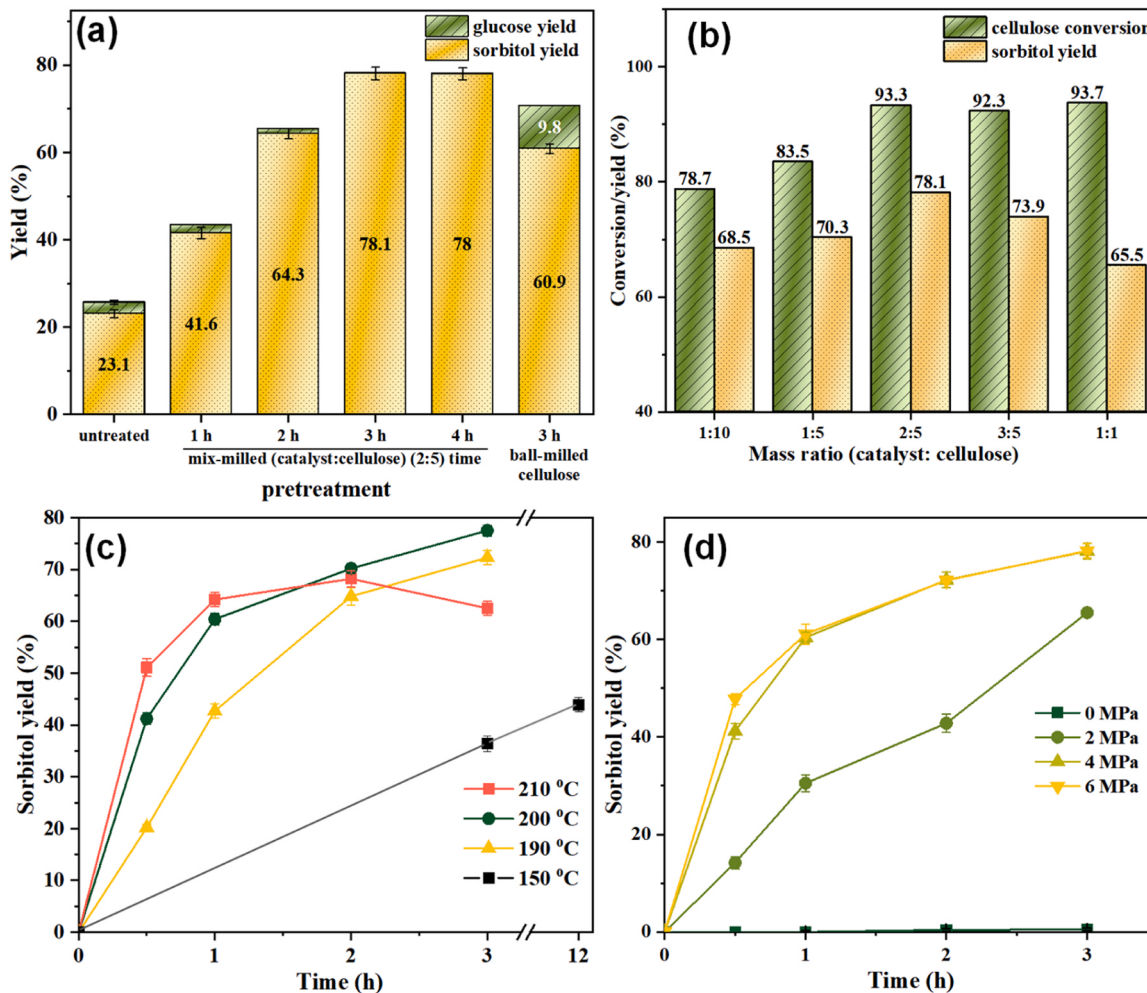


Fig. 5. Effect of reaction conditions on hydrolytic hydrogenation of cellulose in one pot over Ru/P(10)NC-550 catalyst (Reaction conditions unless otherwise stated: 50 mg cellulose, 20 mg catalyst, 5 mL H₂O, 200 °C reaction temperature, 4 MPa partial pressure H₂, 3 h reaction time): (a) variation of pretreatment method; (b) variation of mass ratio of catalyst to cellulose using (5–50) mg catalyst. (c) variation of reaction temperature using 50 mg mix-milled cellulose (d) variation of H₂ partial pressure.

to cellulose substrate was studied (Fig. 5b) and showed that when (catalyst:cellulose) ratio was (2:5), a maximum sorbitol yield was obtained and moreover, when the ratio was further reduced to (1:10), sorbitol yield was still relatively high (68.5%), inferring that the catalyst can be used for high-concentration cellulose reactions. On the other hand, when a high (catalyst:cellulose) ratio of (1:1) was used, sorbitol yields decreased due to formation of by-products (isosorbide, 4.6%) which can be attributed to an excessive number of acid sites.

Water is necessary for cellulose hydrolysis and this requires that the catalyst surface be hydrophilic to ensure its access to the catalytic site [52]. Untreated cellulose had a contact angle with water of 58.2°, while that of ball-milled alone was 38.2°, Contact angle of untreated cellulose with water was 58.2°, which decreased to 38.2° after ball milling of cellulose alone, and further decreased to 27.0° after mix-milling with catalyst, indicating higher hydrophilicity for mix-milled catalyst-cellulose samples (Fig. S12). It is likely that the hydrated hydrogen ions produced by hot-pressing water can fully contact cellulose, resulting in easier access to glycoside bonds. Ball milling enabled the catalyst to fully contact cellulose and allowed phosphate groups to interact with the hydrogen bond network of cellulose [24].

3.2.3. Influence of reaction conditions

The effect of reaction temperature on conversion of cellulose over Ru/P(10)NC-550 catalyst was investigated (Fig. 5c). It can be observed

that the reaction temperature had an important effect on cellulose conversion and sorbitol yield. Within 1 h, by increasing the reaction temperature from 190 °C to 210 °C, the yield of cellulose to sorbitol was significantly increased (Fig. 5c). However, with the extension of reaction time, the yield of sorbitol at 210 °C decreased, with the yield of byproducts increased (C5 sugar alcohols, 9.2% and isopropanol, 2.8%). Conversion of cellulose to sorbitol at lower temperatures was also attempted. After 3 hours of reaction at 150 °C, the cellulose conversion was 44.7%, and the yield of sorbitol was 36.4%, with no by-products detected (Fig. 5c). When the reaction time was extended to 12 h, the yield of sorbitol increased a little with undesirable by-products (isopropanol, 8.5%). Low temperatures lead to insufficient cellulose hydrolysis, and long reaction times lead to further hydrogenation of sorbitol [21].

The effect of H₂ partial pressure was examined on conversion of cellulose over Ru/P(10)NC-550 catalyst at 200 °C (Fig. 5d). In the absence of external H₂, the yield of sorbitol was almost zero after 3 h of reaction, although the yield of glucose reached 50.6% (Fig. S13). The cellulose conversion and sorbitol yield increased with the increase of hydrogen partial pressure from 0 to 6 MPa (Fig. 5d, S13). In particular, we can find that the yield of sorbitol changes almost the same with time as the hydrogen pressure increases from 4 MPa to 6 MPa, only slightly increasing the reaction rate within 0.5 h, which indicated that the hydrogen partial pressure was saturated at 4 MPa (Fig. 5d) [53].

3.2.4. Stability and reusability of Ru/PNC catalysts

Stability and reusability of Ru/PNC catalyst were assessed with cellobiose as substrate to simplify catalyst and product solution separation (Fig. 6). After the first cycle, analysis of the filtrate showed that as much as 0.003 mg/L of Ru and 44.5 mg/L of P had been leached. In run number 2 (Fig. 6) cellobiose seemed to be completely converted and higher sorbitol yields of 94.3% were observed, which infers that oligomers or glucose adsorbed onto the catalyst surface. The increase in sorbitol yields during the first few cycles could be due to the reduction of number of acidic sites on the catalyst due to phosphorus leaching, which improved sorbitol selectivity. Performance of the catalyst with different P content indicated that the optimal acidity-hydrogenation performance ratio of the catalyst with cellobiose as substrates was Ru/P(4)NC-550 (Table S3). In the reaction system with Ru/P(12)NC-550 catalyst, sorbitol used as substrate at relatively high concentrations (8 wt%) underwent conversion into C2-C5 polyols (Fig. S14). After 5 cycles, cellobiose conversion and sorbitol yield decreased and while the Ru content remained almost unchanged at 3 wt% in Ru/P(10)NC (Table S5) and Ru 3p3/2 XPS spectrum remained almost unchanged (Fig. S15), however, P content decreased from 9.8 wt% to 5.9 wt%. Nevertheless, the Ru/P(4)NC-550 maintained its activity for the one-pot conversion of cellobiose to sorbitol (Fig. 6). Although the leaching of phosphate groups under hydrothermal conditions occurred (Table S5, Fig. S16), the presence of nitrogen in Ru/PNC inhibited the degree of metal leaching and the catalyst maintained cycling performance.

3.3. Comparison and analysis of catalytic performance

Compared with many reported catalytic systems, Ru/PNC provided higher yields of sorbitol and specific productivity (Table S6). Previous reports have shown that the hydrolysis rate of cellulose is much lower than the hydrogenation rate of glucose, and the hydrolysis reaction is a rate-limiting step in one-pot conversion schemes [54]. This work achieved a suitable ratio of acid-hydrogenation sites by precise control of elemental P and Ru sites to allow glucose generated from cellulose hydrolysis to be rapidly hydrogenated to sorbitol, which in turn promoted the forward reaction of hydrolysis, maximizing the advantage of a one-pot reaction. Adsorption effects due to mechanochemistry of cellulose substrate with catalyst overcame natural drawbacks of solid-solid heterogeneous systems to a certain extent, thus enhancing hydrolysis

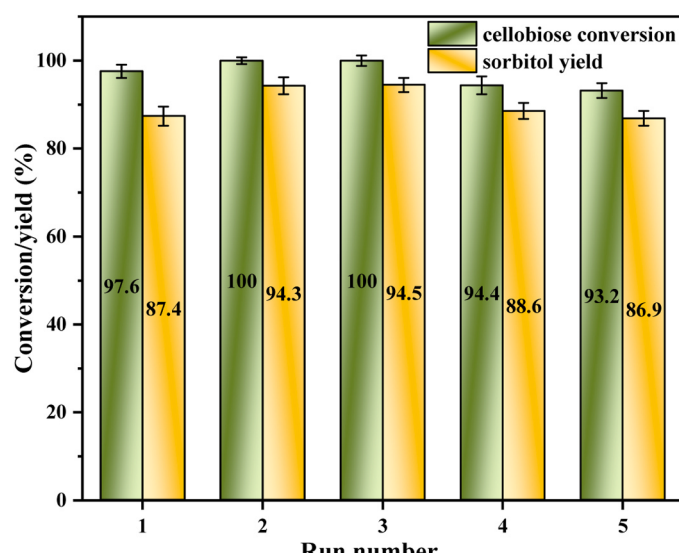


Fig. 6. Recycling of Ru/PNC catalyst for cellobiose conversion to sorbitol. Reaction conditions: cellobiose (1 wt% aqueous solution, 5 mL), 20 mg catalyst, 200 °C reaction temperature, 2 h reaction time for each run, H₂ partial pressure of 4 MPa.

[24]. A schematic for one-pot conversion of cellulose to sorbitol by Ru/PNC (Fig. 7) based on phosphorus content in the catalyst shows that the process can be divided into the following steps: (i) adsorption of cellulose on the catalyst, (ii) cleavage of glycosidic bonds under attack from hydronium ions and acidic group protons resulting in the formation of small sugar molecules and glucose, (iii) ring-opening and hydrogenation of glucose to sorbitol.

As depicted in Fig. 7, the catalyst rich in phosphate groups was in close contact with cellulose, and adsorption of cellulose under external force during mix ball-milling resulted in the destruction of the hydrogen bonding network structure of cellulose. The phosphorylation reaction between glucose and phosphate groups promote glucose ring-opening that readily undergo hydrogenation reactions [55]. At the same time, glucose is rapidly hydrogenated into sorbitol on adjacent exposed Ru sites of the catalyst, which promotes forward movement of the reaction. The weak adsorption ability of the catalyst on sorbitol (Table S4) and appropriate reaction conditions improve reaction selectivity.

In summary, by precisely regulating the acidic sites and hydrogenation sites through cross-linking of a supramolecular assembly with phosphorus groups and adsorption of Ru, the material exhibited stronger hydrophilicity and adsorption to break the limitations of solid-solid mass transfer. Finally, the prepared catalyst was tested with some raw cellulosic materials (cotton wool, filter paper) and sorbitol yields as high as 70% could be realized. The results confirm that the Ru/PNC catalyst has high selectivity, good recyclability, and uses simple operations for its preparation, thus it has high potential for practical industrial use.

4. Conclusions

In this work, nitrogen rich chitosan and phosphorus rich phytic acid were used as biomass resources to cross-link and coordinate Ru for preparing Ru/PNC bifunctional catalysts with controllable acidity and hydrogenation sites. Through surface modification and functionalization, bifunctional catalysts were synthesized and when they were applied with mechanochemical pretreatment, limitations for solid-solid catalyst:substrate mass transfer could be overcome. Using pure water, cellulose substrate with Ru/PNC catalyst could be converted in one-pot to obtain sorbitol yields as high as 78%. Catalyst to substrate mass ratios (catalyst:cellulose) as low as (1:10) gave sorbitol yields as high as 68% showing that the material has potential application for large-scale reaction systems. The prepared catalyst showed good reusability and could be recycled for at least five times. The proposed supramolecular assembly and crosslinking method for catalyst synthesis is sustainable based on its use of renewable resources, it is reliable based on procedures used that are all simple, and it is versatile, based on precise control of acid sites and hydrogenation sites of the material. The proposed supramolecular assembly and crosslinking method has a broad scope for synthesis of catalysts having specific sites required for conversion of biomass-related substrates.

CRediT authorship contribution statement

Richard L Smith: Writing – review & editing, Methodology, Formal analysis, Conceptualization. **Xinhua Qi:** Writing – review & editing, Supervision, Resources, Project administration, Methodology, Funding acquisition, Formal analysis, Conceptualization. **Yingqiao Zhou:** Writing – original draft, Visualization, Validation, Software, Methodology, Investigation, Formal analysis, Data curation, Conceptualization.

Declaration of Competing Interest

The authors declare that they have no known competing financial interests or personal relationships that could have appeared to influence the work reported in this paper.

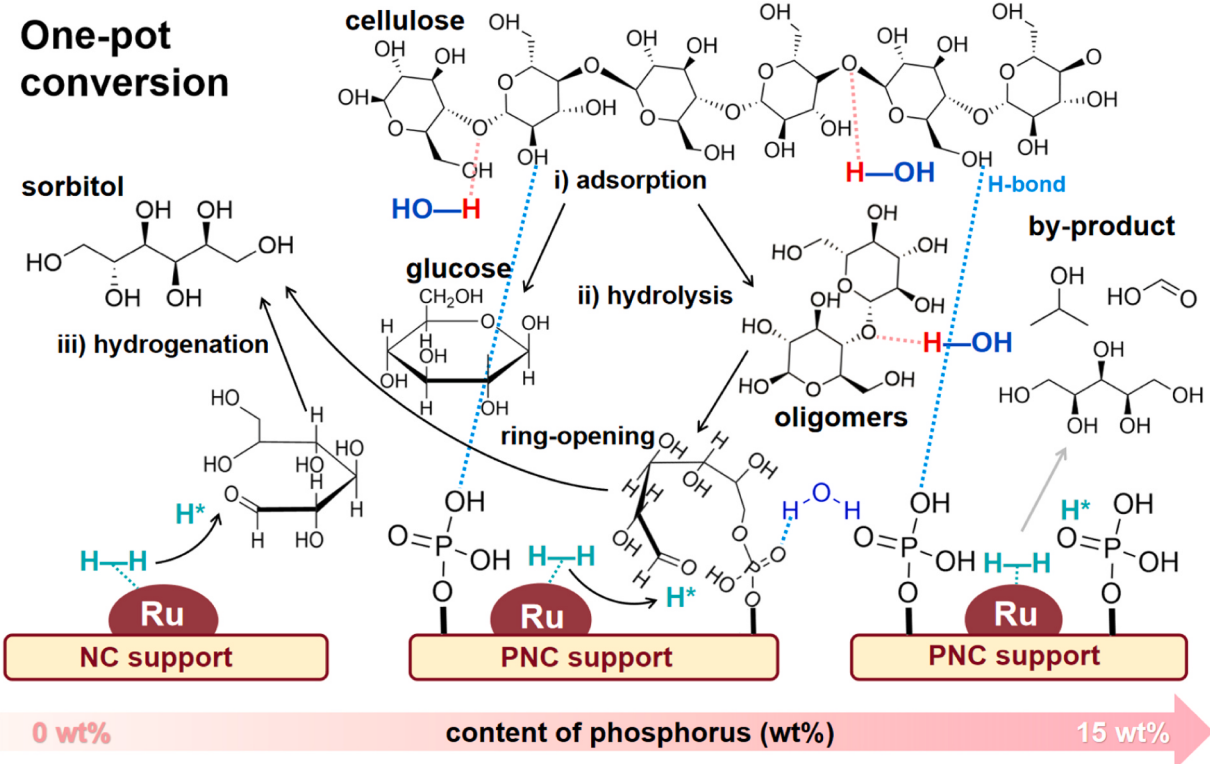


Fig. 7. Schematic mechanism of one-pot conversion from cellulose to sorbitol over Ru/PNC catalyst.

Data Availability

Data will be made available on request.

Acknowledgments

This work was financially supported by the National Natural Science Foundation of China (No. 22178181), the Natural Science Fund of Tianjin (No. 21JCZDJC00180) and the Fundamental Research Funds for the Central Universities (Nankai University (No. 63243129)).

Appendix A. Supporting information

Supplementary data associated with this article can be found in the online version at [doi:10.1016/j.apcatb.2024.124217](https://doi.org/10.1016/j.apcatb.2024.124217).

References

- [1] R. Mori, Replacing all petroleum-based chemical products with natural biomass-based chemical products: a tutorial review, *RSC Sustain.* 1 (2) (2023) 179–212.
- [2] R. Fang, A. Dhakshinamoorthy, Y. Li, H. Garcia, Metal organic frameworks for biomass conversion, *Chem. Soc. Rev.* 49 (11) (2020) 3638–3687.
- [3] A. Shrotri, H. Kobayashi, A. Fukuoka, Cellulose depolymerization over heterogeneous catalysts, *Acc. Chem. Res.* 51 (3) (2018) 761–768.
- [4] W. Deng, Y. Feng, J. Fu, H. Guo, Y. Guo, B. Han, Z. Jiang, L. Kong, C. Li, H. Liu, P.T. T. Nguyen, P. Ren, F. Wang, S. Wang, Y. Wang, Y. Wang, S.S. Wong, K. Yan, N. Yan, X. Yang, Y. Zhang, Z. Zhang, X. Zeng, H. Zhou, Catalytic conversion of lignocellulosic biomass into chemicals and fuels, *Green. Energy Environ.* 8 (1) (2023) 10–114.
- [5] J. Dharmaraja, S. Shobana, S. Arvindnarayanan, R.R. Francis, R.B. Jeyakumar, R.G. Saratale, V. Ashokkumar, S.K. Bhatia, V. Kumar, G. Kumar, Lignocellulosic biomass conversion via greener pretreatment methods towards biorefinery applications, *Bioresour. Technol.* 369 (2023) 128328.
- [6] M. Zeng, X. Pan, Insights into solid acid catalysts for efficient cellulose hydrolysis to glucose: progress, challenges, and future opportunities, *Catal. Rev.* (1) (2020) 1–46.
- [7] M.J. Ahmed, B.H. Hameed, Hydrogenation of glucose and fructose into hexitols over heterogeneous catalysts: a review, *J. Taiwan Inst. Chem. Eng.* 96 (2019) 341–352.
- [8] H. Kobayashi, H. Ohta, A. Fukuoka, Conversion of lignocellulose into renewable chemicals by heterogeneous catalysis, *Catal. Sci. Technol.* 2 (5) (2012) 869–883.
- [9] A. Fukuoka, P.L. Dhepe, Catalytic conversion of cellulose into sugar alcohols, *Angew. Chem.* 45 (31) (2006) 5161–5163.
- [10] J. Zhang, J.-b Li, S.-B. Wu, Y. Liu, Advances in the catalytic production and utilization of sorbitol, *Ind. Eng. Chem. Res.* 52 (34) (2013) 11799–11815.
- [11] W. Deng, X. Tan, W. Fang, Q. Zhang, Y. Wang, Conversion of cellulose into sorbitol over carbon nanotube-supported ruthenium catalyst, *Catal. Lett.* 133 (1) (2009) 167.
- [12] L. Lin, X. Han, B. Han, S. Yang, Emerging heterogeneous catalysts for biomass conversion: studies of the reaction mechanism, *Chem. Soc. Rev.* 50 (20) (2021) 11270–11292.
- [13] Y. Wu, H. Wang, J. Peng, M. Ding, Advances in catalytic valorization of cellulose into value-added chemicals and fuels over heterogeneous catalysts, *Catal. Today* 408 (2023) 92–110.
- [14] B. Zhang, X. Li, Q. Wu, C. Zhang, Y. Yu, M. Lan, X. Wei, Z. Ying, T. Liu, G. Liang, Synthesis of Ni/mesoporous ZSM-5 for direct catalytic conversion of cellulose to hexitols: modulating the pore structure and acidic sites via a nanocrystalline cellulose template, *Green. Chem.* 18 (11) (2016) 3315–3323.
- [15] X. Liu, X. Liu, N. Li, P. Ma, Y. Zhang, Direct synthesis of hexitols from microcrystalline cellulose and birch over zirconium(IV) phosphate supported nickel catalysts and the mechanism study, *Green. Chem.* 23 (3) (2021) 1353–1360.
- [16] N.V. Gromov, T.B. Medvedeva, O.P. Taran, M.N. Timofeeva, O. Said-Aizpuru, V.N. Panchenko, E.Y. Gerasimov, I.V. Kozhevnikov, V.N. Parmon, The main factors affecting the catalytic properties of Ru/Cs-HPA systems in one-pot hydrolysis-hydrogenation of cellulose to sorbitol, *Appl. Catal. A: Gen.* 595 (2020) 117489.
- [17] N.V. Gromov, T.B. Medvedeva, Y.A. Rodikova, M.N. Timofeeva, V.N. Panchenko, O.P. Taran, I.V. Kozhevnikov, V.N. Parmon, One-pot synthesis of sorbitol via hydrolysis-hydrogenation of cellulose in the presence of Ru-containing composites, *Bioresour. Technol.* 319 (2021) 124122.
- [18] Y. Zhang, G. Zhang, T. Chen, Efficient one-pot conversion of cellulose to sorbitol over Ni-based carbon catalysts with embedment structure, *Fuel* 339 (2023) 127447.
- [19] L.S. Ribeiro, J.J.M. Órfão, M.F.R. Pereira, An overview of the hydrolytic hydrogenation of lignocellulosic biomass using carbon-supported metal catalysts, *Mater. Today Sustain.* 11–12 (2021) 100058.
- [20] N. Rey-Raap, L.S. Ribeiro, J.J. d M. Órfão, J.L. Figueiredo, M.F.R. Pereira, Catalytic conversion of cellulose to sorbitol over Ru supported on biomass-derived carbon-based materials, *Appl. Catal. B: Environ.* 256 (2019) 117826.
- [21] Z. Li, Y. Liu, C. Liu, S. Wu, W. Wei, Direct conversion of cellulose into sorbitol catalyzed by a bifunctional catalyst, *Bioresour. Technol.* 274 (2019) 190–197.
- [22] Q. Liu, H. Wang, H. Xin, C. Wang, L. Yan, Y. Wang, Q. Zhang, X. Zhang, Y. Xu, G. W. Huber, L. Ma, Selective cellulose hydrogenolysis to ethanol using Ni@C combined with phosphoric acid catalysts, *ChemSusChem* 12 (17) (2019) 3977–3987.

[23] J. Zhang, S. Wu, B. Li, H. Zhang, Direct conversion of cellobiose into sorbitol and catalyst deactivation mechanism, *Catal. Commun.* 29 (2012) 180–184.

[24] Y. Dai, M. Geng, Y. Tao, Z. Zhang, C. Feng, J. Huang, F. Liu, H. Na, J. Zhu, Hydrolysis of cellulose to glucose in aqueous phase with phosphate group modified hydroxy-rich carbon-based catalyst, *Carbon* 206 (2023) 72–83.

[25] Z. Wu, S. Ge, C. Ren, M. Zhang, A. Yip, C. Xu, Selective conversion of cellulose into bulk chemicals over Brønsted acid-promoted ruthenium catalyst: one-pot vs. sequential process, *Green. Chem.* 14 (12) (2012) 3336–3343.

[26] Y. Yang, S. Shao, F. Yang, D.L. Brewe, S. Guo, D. Ren, S. Hao, Conversion of cellulose to high-yield glucose in water over sulfonated mesoporous carbon fibers with optimized acidity, *Green. Chem.* 23 (12) (2021) 4477–4489.

[27] I.O. Saheed, W.D. Oh, F.B.M. Suah, Chitosan modifications for adsorption of pollutants – A review, *J. Hazard. Mater.* 408 (2021) 124889.

[28] X.-W. Cheng, J.-P. Guan, X.-H. Yang, R.-C. Tang, F. Yao, A bio-resourced phytic acid/chitosan polyelectrolyte complex for the flame retardant treatment of wool fabric, *J. Clean. Prod.* 223 (2019) 342–349.

[29] Q. Xia, T. Zhu, Z. Chai, Y. Wang, TFC membrane with in-situ crosslinked ultrathin chitosan layer for efficient water/ethanol separation enabled by multiple supramolecular interactions, *Adv. Membr.* 3 (2023) 100062.

[30] H. Wu, Z. Chen, Y. Wang, E. Cao, F. Xiao, S. Chen, S. Du, Y. Wu, Z. Ren, Regulating the allocation of N and P in codoped graphene via supramolecular control to remarkably boost hydrogen evolution, *Energy Environ. Sci.* 12 (9) (2019) 2697–2705.

[31] Q. Liang, Q. Li, L. Xie, H. Zeng, S. Zhou, Y. Huang, M. Yan, X. Zhang, T. Liu, J. Zeng, K. Liang, O. Terasaki, D. Zhao, L. Jiang, B. Kong, Superassembly of surface-enriched Ru nanoclusters from trapping–bonding strategy for efficient hydrogen evolution, *ACS Nano* 16 (5) (2022) 7993–8004.

[32] W. Wang, H. Zhang, Y. Wang, F. Zhou, Zhiyu Xiang, W. Zhu, H. Wang, , P-induced electron transfer interaction for enhanced selective hydrogenation rearrangement of furfural to cyclopentanone, *J. Energy Chem.* 92 (2024) 43–51.

[33] J. Zhang, Z. Zhao, Z. Xia, L. Dai, A metal-free bifunctional electrocatalyst for oxygen reduction and oxygen evolution reactions, *Nat. Nanotechnol.* 10 (5) (2015) 444–452.

[34] J. Shi, M. Zhao, Y. Wang, J. Fu, X. Lu, Z. Hou, Upgrading of aromatic compounds in bio-oil over ultrathin graphene encapsulated Ru nanoparticles, *J. Mater. Chem. A* 4 (16) (2016) 5842–5848.

[35] W. Li, H. Zhang, K. Zhang, W. Hu, Z. Cheng, H. Chen, X. Feng, T. Peng, Z. Kou, Monodispersed ruthenium nanoparticles interfacially bonded with defective nitrogen-and-phosphorus-doped carbon nanosheets enable pH-universal hydrogen evolution reaction, *Appl. Catal. B: Environ.* 306 (2022) 121095.

[36] Z.-J. Diao, L.-Q. Huang, B. Chen, T. Gao, Z.-Z. Cao, X.-D. Ren, S.-J. Zhao, S. Li, Amorphous Ni-Ru bimetallic phosphide composites as efficient catalysts for the hydrogenolysis of diphenyl ether and lignin, *Fuel* 324 (2022) 124489.

[37] S. Zhang, Y. Rui, X. Zhang, R. Sa, F. Zhou, R. Wang, X. Li, Ultrafine cobalt-ruthenium alloy nanoparticles induced by confinement effect for upgrading hydrogen evolution reaction in all-pH range, *Chem. Eng. J.* 417 (2021) 128047.

[38] Z. Li, J. Lin, B. Li, C. Yu, H. Wang, Q. Li, Construction of heteroatom-doped and three-dimensional graphene materials for the applications in supercapacitors: a review, *J. Energy Storage* 44 (2021) 103437.

[39] A. Jaleel, A. Haider, Van Nguyen, C. Lee, K.R. Choung, S. Han, J.W. Baek, S.-H. Shin, C.-H. Jung, K.-D, Structural effect of Nitrogen/Carbon on the stability of anchored Ru catalysts for CO₂ hydrogenation to formate, *Chem. Eng. J.* 433 (2022) 133571.

[40] M. Cheng, Y. Zhang, B. Lai, L. Wang, S. Yang, K. Li, D. Wang, Y. Wu, G.-H. Chen, J. Qian, Nitrogen and phosphorus co-doped porous carbons (NPCs) for peroxydisulfate (PDS) activation towards tetracycline degradation: Defects enhanced adsorption and non-radical mechanism dominated by electron transfer, *Chem. Eng. J.* 455 (2023) 140615.

[41] H. Wang, C. Xu, Q. Chen, M. Ming, Y. Wang, T. Sun, Y. Zhang, D. Gao, J. Bi, G. Fan, Nitrogen-doped carbon-stabilized Ru nanoclusters as excellent catalysts for hydrogen production, *ACS Sustain. Chem. Eng.* 7 (1) (2019) 1178–1184.

[42] R. Wang, D. Li, T. Li, W. Sun, W. Hu, Crystalline-amorphous Ru@RuP core-shell nanoparticles anchored on carbon nanotube for enhanced hydrogen evolution electrocatalysis, *Colloids Surf. A: Physicochem. Eng. Asp.* 668 (2023) 131452.

[43] Y. Yang, D. Ren, C. Shang, Z. Ding, X. Luo, Site isolated Ru clusters and sulfoacids in a yolk-shell nanoreactor towards cellulose valorization to 1,2-propylene glycol, *Chem. Eng. J.* 452 (2023) 139206.

[44] P.A. Lazaridis, S. Karakoula, A. Delimitis, S.M. Coman, V.I. Parvulescu, K. S. Triantafyllidis, d-Glucose hydrogenation/hydrogenolysis reactions on noble metal (Ru, Pt)/activated carbon supported catalysts, *Catal. Today* 257 (2015) 281–290.

[45] H. Nakayama, T. Eguchi, N. Nakamura, S. Yamaguchi, M. Danjyo, M. Tsuhako, Structural study of phosphate groups in layered metal phosphates by high-resolution solid-state ³¹P NMR spectroscopy, *J. Mater. Chem. B* 7 (6) (1997) 1063–1066.

[46] H. Zhang, S. Wang, H. Zhang, J.H. Clark, F. Cao, A biomass-derived metal-free catalyst doped with phosphorus for highly efficient and selective oxidation of furfural into maleic acid, *Green. Chem.* 23 (3) (2021) 1370–1381.

[47] A. Zheng, S.-B. Liu, F. Deng, ³¹P NMR chemical shifts of phosphorus probes as reliable and practical acidity scales for solid and liquid catalysts, *Chem. Rev.* 117 (19) (2017) 12475–12531.

[48] R. Fu, L. Liu, W. Huang, P. Sun, Studies on the structure of activated carbon fibers activated by phosphoric acid, *J. Appl. Polym. Sci.* 87 (14) (2003) 2253–2261.

[49] Y. Zhou, R.L. Smith Jr., X. Qi, Chemocatalytic production of sorbitol from cellulose via sustainable chemistry – a tutorial review, *Green. Chem.* 26 (1) (2024) 202–243.

[50] B. Yu, Z. Zhang, W. Liu, F. Liu, J. Huang, H. Na, J. Zhu, Hydroxyl-enriched core-shell carbon nanotubes for catalytic hydrolysis of regenerated cellulose to glucose, *ACS Appl. Nano Mater.* 5 (4) (2022) 5364–5372.

[51] A. Gabe, A. Takatsuki, M. Hiratani, M. Kaneeda, Y. Kurihara, T. Aoki, H. Mashima, T. Ishii, J.-I. Ozaki, H. Nishihara, T. Kyotani, In-depth analysis of key factors affecting the catalysis of oxidized carbon blocks for cellulose hydrolysis, *ACS Catal.* 12 (2) (2022) 892–905.

[52] M. Kitano, D. Yamaguchi, S. Saganuma, K. Nakajima, H. Kato, S. Hayashi, M. Hara, Adsorption-enhanced hydrolysis of β -1,4-Glucan on graphene-based amorphous carbon bearing SO₃H, COOH, and OH groups, *Langmuir* 25 (9) (2009) 5068–5075.

[53] J. Xi, Y. Zhang, Q. Xia, X. Liu, J. Ren, G. Lu, Y. Wang, Direct conversion of cellulose into sorbitol with high yield by a novel mesoporous niobium phosphate supported Ruthenium bifunctional catalyst, *Appl. Catal. A: Gen.* 459 (2013) 52–58.

[54] L. Negahdar, J.U. Oltmanns, S. Palkovits, R. Palkovits, Kinetic investigation of the catalytic conversion of cellobiose to sorbitol, *Appl. Catal. B: Environ.* 147 (2014) 677–683.

[55] X. Zhang, L.J. Durnell, M.A. Isaacs, C.M.A. Parlett, A.F. Lee, K. Wilson, Platinum-catalyzed aqueous-phase hydrogenation of d-Glucose to d-Sorbitol, *ACS Catal.* 6 (11) (2016) 7409–7417.